



## Switching algorithms for extending battery life in Electric Vehicles

Ron Adany<sup>a,\*</sup>, Doron Aurbach<sup>b</sup>, Sarit Kraus<sup>a</sup>

<sup>a</sup> Department of Computer Science, Bar-Ilan University, Ramat-Gan 52900, Israel

<sup>b</sup> Department of Chemistry, Bar-Ilan University, Ramat-Gan 52900, Israel

### HIGHLIGHTS

- ▶ A battery's life is greatly affected by the method of use.
- ▶ Discharging in non-optimal currents has negative effects on the battery's life.
- ▶ We propose advanced switching algorithms to minimize these effects.
- ▶ The battery's life can be significantly extended by the proposed algorithms.

### ARTICLE INFO

#### Article history:

Received 27 July 2012

Received in revised form

16 December 2012

Accepted 18 December 2012

Available online 27 December 2012

#### Keywords:

Electric Vehicles (EV)

Switching algorithms

Battery life

Lithium ion batteries

Battery Management System (BMS)

### ABSTRACT

The battery is a key component in any Electric Vehicle (EV) and its method of operation may have a tremendous effect on its life. In this paper we focus on improving the battery's life. Each battery is a pack of cells designed to be discharged and charged with specific optimal currents, whereby other currents, i.e. higher or lower than the optimal currents, may have negative effects on its life. We model these negative effects as penalties that are aggregate over time and propose a discharge method to minimize them. The common discharge method is very simple but far from optimal since the current demand is supplied using all the battery's cells where the current from each is the same. The method we propose is advanced switching algorithms that select a subset of the battery's cells for each current demand and control the discharge current from each, based on the electrochemical properties of the individual cells. We evaluate our proposed algorithms using simulations on world-wide driving cycles. The results reveal that compared to the common discharge method almost all penalties can be eliminated and the battery's life can be significantly extended.

© 2012 Elsevier B.V. All rights reserved.

## 1. Introduction

Electric Vehicles (EVs) are the next generation of cars in the world of automobiles. The propulsion solutions for EVs are based on hybrid or fully battery powered electric vehicles [1]. The critical part of EVs, that determine their performance, is the battery [2]. In this work we focus on one of its problems, namely the battery's life.

The life of operating batteries is usually measured as the number of cycles, that can be obtained, until the capacity per cycle declines beyond a pre-determined threshold [3]. The energy extracted from the battery during full discharge is the integration of voltage as a function of capacity throughout the discharge process, until its cut off point (measured in Watt-hours). However, an alternative definition, which we use throughout this paper, can be the total accumulated energy extracted from a battery during its life.

Batteries are very expensive [4] and hence it is critically important to prolong their life as much as possible. The method of operating the EV battery may have a dominant effect on its life. According to results presented in Ref. [5] operating it incorrectly might reduce the battery's life to even a third of its expected duration. Thus, it is logical that the Battery Management System (BMS) in the EV includes a component that will control the battery's operation in order to extend its life.

An EV battery is actually a pack of strings of cells connected in a series, in order to reach the required high voltage. These strings of cells, i.e. cell-series, are connected in parallel, in order to provide the required current. For safety reasons, e.g. issues related to heat dissipation during operation, it is important to construct such large batteries from small individual cells. Thus, the focus in this paper is on the level of the individual cell-series in the battery, which determine the total voltage of the battery.

Developments in the Lithium-ion (Li-ion) battery technology in the last decade have made Li-ion batteries the standard choice of power sources for EVs [6,7]. Thus, in this paper we focus on Li-ion

\* Corresponding author. Tel.: +972 3 5318866; fax: +972 3 7384056.

E-mail addresses: [adanyr@cs.biu.ac.il](mailto:adanyr@cs.biu.ac.il) (R. Adany), [aurbach@mail.biu.ac.il](mailto:aurbach@mail.biu.ac.il) (D. Aurbach), [sarit@cs.biu.ac.il](mailto:sarit@cs.biu.ac.il) (S. Kraus).

batteries. Based on the chemistry and engineering of Li-ion batteries, it is clear that the values of the current upon discharge of a single cell and cell-series, i.e. the rate of operation, may have a significant impact on the battery's life. The use of discharge currents that are too low or too high, may have a detrimental effect on the battery's life, as shall be discussed later in Section 3.2. These effects justify the optimization efforts described in this paper. Based on these insights we propose a penalty function, which for each discharge current, defines a penalty in terms of the detrimental effect on the battery's life.

The motivation for our research emerges from the possibility of extending the life of EV batteries via their smart operation. The discharge method that is commonly used for EV batteries, presented in Section 4.1, is very simple as the current demand is supplied using all cells in the battery simultaneously, hence the load is equally divided among them. The rationale behind this method is simplicity of implementation and the assumption that the lower the current drawn from each cell in the battery the better. However, as described in Section 3.2, the behavior and performance of a real battery is more complex, and this assumption is not always true.

In this paper we focus on optimizing the process of smart distribution of the load of each demand over the cells in the EV battery. Our main theory is that not all the cell-series in the battery should be discharged together but rather, each time only part of them should be discharged. We propose advanced switching algorithms that select the cell-series to be discharged for each current demand and control the discharge current drawn from each.

The rest of this paper is organized as follows. In Section 2 we provide an overview of related work on switching methods. We formally describe the problem in Section 3. Our proposed switching algorithms are presented in Section 4. A description of the simulation data we used to evaluate our algorithms is provided in Section 5. The simulation results are presented in Section 6 and discussed in Section 7. Finally we present our conclusions and direction for future work in Section 8.

**2. Related work**

The subject of battery management for multiple battery systems has been widely studied. Most of the studies were intended to maximize the battery lifetime, i.e. the time until most of the cells in the battery have lost an essential part of their capacity in the course of prolonged cycling. Basically there are two kinds of discharge algorithms: sequential and parallel. In the sequential algorithms only one battery supplies the workload each time, while in the parallel algorithms a subset of batteries supplies the workload each time.

Sequential discharging algorithms for lifetime maximization of systems with multiple identical batteries were proposed and tested in Ref. [8]. The proposed algorithms include: (i) serial – discharging each battery until it is emptied and then discharging the next battery; (ii) static switching – discharging each battery for a certain amount of time then moving to the next battery; and (iii) dynamic switching – discharging each battery for a different amount of time depending on its physical state, e.g. remaining capacity.

In Ref. [8], the lifetime of a multiple batteries system was compared to the lifetime of a monolithic battery, i.e. a single battery with a capacity equal to the sum of all the batteries. Static and dynamic algorithms were found to significantly increase the lifetime and close the gap compared to a monolithic battery. Following their results, we realized the need for dynamic algorithms which determine the next discharge schedule based on the cells' state.

Parallel discharging algorithms, with and without sequential switching, for systems with multiple identical batteries were discussed in Ref. [9]. According to the analytic results presented in their paper, when using parallel discharging algorithms the lifetime

of a multiple batteries system is equal to that of a monolithic battery and not less than that when using sequential algorithms. In addition, they reported that the lifetime of batteries operated by any switching algorithm becomes very similar to that of a monolithic battery, as the switching frequency increases.

The current demands in EVs are not known in advance and may be provided using prediction methods based on the route, driving profile, history of demands, etc. In Ref. [10] discharge methods among multiple batteries were discussed. There were  $N$  batteries and  $M$  current levels with their distribution over time, i.e. the current demand values were known in advance but the actual sequence was not. The objective was to extend the lifetime of the batteries. In Ref. [11] an Energy Management (EM) system for Hybrid Electric Vehicles was discussed where the future demands are unknown. An online EM strategy was presented and evaluated by simulations. Throughout this paper we assume that only the next demand, i.e. the current that needs to be supplied, is known. In this sense our algorithms can be considered online strategies.

**3. Problem description**

The problem is defined as follows. The battery pack consists of  $m$  identical cell-series,  $s_1, s_2, \dots, s_m$ , all having the same initial capacity  $C$ . There are  $n$  current demands,  $d_1, d_2, \dots, d_n$ , where  $d_i$  is the required current in amperes (A) for the  $i$ -th second. The sequence of the current demands, and in particular its length  $n$ , is not known in advance. However, the total capacity of the cell-series is guaranteed to satisfy all demands, i.e.  $\sum_{i=1}^n d_i \leq mC$ . A summary of the notations is presented in Table 1.

The voltage of batteries usually changes during the discharging and the charging processes. The voltage profile of Li-ion batteries depends on the type of Li-ions intercalation process. It may slope, if the Li intercalation forms a solid solution. If Li intercalation occurs via first order phase transition, the voltage profile may be flat (plateau), changing only at the beginning and end of the process.

One of the promising batteries technology for electric mobility applications is graphite LiFeO<sub>4</sub> in which both the negative and positive materials intercalate with Li ions via first order phase transitions. Thereby, their voltage profile is relatively flat. In this study, we refer to the above battery system and thus we approximated the voltage as constant. Such an assumption is not real, as the voltage profile of graphite LiFePO<sub>4</sub> batteries is not fully flat, but rather has some steps [12]. Nevertheless, as a first approximation, that facilitates the calculations, it should be considered very reasonable. The model can then be adjusted to include all types of voltage profiles (beyond the scope of the present study).

Consequently, the voltage of all cell-series is considered to be the same and equal to  $V$ . In addition, the voltage of all demands is assumed to be fixed and equal to  $V$ .

The entire operation process is as follows. The current demands are given one by one to the switching algorithm as well as the states

**Table 1**  
Notation and terms summary.

Cell-series	$s_1, s_2, \dots, s_j, \dots, s_m$
$C$	The initial capacity of all cell-series.
$c_j^i$	The capacity of cell-series $j$ before demand $i$ .
$I_{OPT}$	The optimal discharge current of the cell-series. Throughout this paper we assume that $I_{OPT} = 1$ .
Current demands	$d_1, d_2, \dots, d_i, \dots, d_n$
$d_i$	The current demand for the $i$ -th second.
Decision variables	
$I_j^i$	The discharge current of cell-series $j$ for demand $i$ .

of all cell-series. In other words, every second a current demand,  $d_i$ , is given in addition to the remaining capacity of the cell-series,  $c_j^i$ .

The  $i$ -th demand can be satisfied in various ways. Any allocation of  $d_i$  from the cell-series is acceptable, and there are no constraints regarding the distribution of  $d_i$  among the cell-series. Our objective is to minimize the total penalty of the cell-series, i.e. to maximize the life of the entire battery pack. Thus, the goal is to determine the values  $I_j^i$ , where  $I_j^i$  is the discharge current of cell-series  $s_j$  to supply the current demand  $i$ .

Each allocation is associated with a penalty as there are 'good' and 'bad' allocations – since an optimal discharge current exists. All the cell-series have the same optimal discharge current value  $I_{OPT}$ . This value should be determined by analysis of the electrochemical properties of the cells' chemistry.

In this section we first present the mathematical model of the problem in Section 3.1; in Section 3.2 we provide the optimal current operation of the battery; and in Section 3.3 we discuss the penalty function.

### 3.1. Mathematical model

In this section we present the mathematical model of a case of the problem in which all current demands are known in advance. While this is not the case in practice, such a model can be used as a baseline for defining the problem with which we are confronted. The mathematical model can be presented as follows.

$$\begin{aligned} \min \quad & \sum_{i=1}^n \sum_{j=1}^m \text{Penalty}(I_j^i) \\ \text{s.t.} \quad & \sum_{i=1}^n I_j^i \leq C \quad \forall j = 1 \dots m \\ & \sum_{j=1}^m I_j^i = d_i \quad \forall i = 1 \dots n \\ & 0 \leq I_j^i, I_j^i \in R \quad \forall i = 1 \dots n, j = 1 \dots m \end{aligned} \quad (1)$$

The objective function in the mathematical model is to minimize the total penalty of allocating currents from the cell-series. The first constraint ensures that cell-series  $j$  has enough capacity, i.e. it does not over allocate. The second constraint requires that demand  $d_i$  is satisfied by the discharges of the cell-series. The last two constraints make our decision variables real and non-negative numbers.

### 3.2. Optimal current operation

The discharge current has a tremendous effect on the cell-series and is a key factor in the battery's life. It is well known that the use of high currents causes the cell-series capacity to progressively decrease from the nominal value [13,14]. In addition, it is known that the efficiency of the cell-series decreases when the average discharge current increases [15].

According to experiments reported in Ref. [5] for a rechargeable Li/MoS<sub>2</sub> cell, there is a strong dependency between the discharge current and the degradation mechanisms that affect a battery's life. According to their results, the effect of discharging a non-optimal current might lead to a decrease of up to third of the battery's life. In addition, their experiments show that high discharge currents cause cathode degradation that leads to cathode failure, while low currents cause electrolyte degradation that leads to anode failure. Moreover, a maximum life was found for some current, which seems to be the optimal discharge current for the battery.

Li-ion batteries are based on reversible Lithium (Li) ion intercalation reactions with inorganic hosts, occurring at high (the positive, cathode side) and low (the negative, anode side) red-ox

potentials. In all practical Li-ion batteries, the electrodes and the electrolyte solutions never reach thermodynamic stability. These systems function under meta-stable conditions due to the passivation phenomena.

The most important negative electrode materials are graphite type carbons. Graphite reversibly intercalates Li ions at potentials between 250 and 20 mV vs Li, up to a stoichiometry of LiC<sub>6</sub> [16]. Li-graphite intercalation compounds are highly reactive with any polar-aprotic Li ions containing a solution that can be suitable for battery application. Most of the relevant solvents (e.g. alkyl carbonates, esters, ethers) and salt anions of the MX<sub>y</sub>-type (M = P, Cl, B; X = O, F) are reduced at potentials below 1.5 V vs Li [17].

Fortunately, in most cases, the reduction products precipitate as insoluble surface films comprising ionic Li compounds. These surface films behave like solid electrolyte interphases (SEI) that passivate the electrodes electronically but allow free Li ions to transport through them under an electrical field [18]. Graphitic materials are very fragile and soft. They easily exfoliate upon insertion of solvated Li ions if the surface films on them do not force the Li ions to dissolve and migrate through them completely naked, under the applied electrical field, into the active mass [19].

If the passivation of graphite electrodes is not effective enough, solution species drugged with the intercalating Li ions, are forced to enter into the graphite particles and are reduced therein. If these reactions occur, they completely destroy the graphite particles, whereby they are no longer effective electrode materials [20]. The cathode materials in Li-ion batteries are mostly Li<sub>x</sub>MO<sub>y</sub> (layered or spinel structures) or Li<sub>x</sub>MPO<sub>4</sub> (olivine structure) where M is transition metal or a mixture of transition metal cations (Ni, Co, Fe, Mn, V, etc.). With these cathode materials, intrinsic unstable situations are due to several possible reactions, that also form surface films [21]. The latter may provide stable passivation to these cathode materials in solutions, or detrimentally affect Li ions transport from the solution to the active mass (i.e. introducing high impedance).

The reactions on the cathode side include acid–base interactions, nucleophilic reactions of the basic, negatively charged surface oxygen atoms on the electrophilic solvent molecules (such as alkyl carbonates), oxidation of solution species (if the red-ox voltage required for the Li intercalation–de-intercalation reactions is too high) and dissolution of transition metal cations to the solution phase [22]. The latter process is very detrimental for Li-ion batteries, because such cations migrate to the anode, are reduced then to form metallic clusters, which destroy the passivation of graphite electrodes [23]. Hence, all kinds of Li-ion batteries have to operate under delicate metastable situations, maintained by very complicated passivation phenomena.

Moreover, insertion of Li ions into most host materials (both graphite and Li<sub>x</sub>MO<sub>y</sub> compounds) leads to some volume increase of the active mass, that challenges its passivation by the surface films (they have to be flexible enough to accommodate the particle expansion upon Li ions insertion). Thereby, application of overly intensive driving forces, namely a current density that is too high, for these Li insertion electrodes may destroy their passivation [24]. Also, currents that are too high may lead to Li metal deposition on graphite and to the formation of highly reactive Li dendrites that endanger the safety of the cells [25]. Hence it is clear that the currents drawn from Li insertion electrodes should have upper limits.

The above described electrode-solutions' meta-stability under which Li-ion batteries have to function, leads to the situation whereby working currents that are too low, can also negatively affect the stability of Li-ion batteries. As explained below, the most problematic state of Li-ion batteries in terms of thermodynamic stability, i.e. most remote from the equilibrium condition, is when they are fully charged. In this state, the anode possesses the highest reduction ability and the cathode possesses the maximal ability of

oxidation of solution species. Nevertheless, Li-ion batteries have to be stored at their fully charged state, in order to deliver their entire capacity upon demand.

When these batteries are stored at rest (static situation) in their fully charged state, they are usually well protected from detrimental side effects by the above mentioned passivation (due to the existence of protective surface films on both electrodes). However, as the batteries start to work in their fully charged state, thus moving in this sensitive situation from static to dynamic conditions, the electrodes passivation becomes much weaker in the dynamic state. Hence, it is logical not to operate the batteries at currents that are too low (thus leaving them in the dynamic state, which is a highly sensitive state of being nearly fully charged for too long), but rather drawing high enough currents that will bring the batteries quickly to partially charged states, in which the driving force of detrimental side effects is much lower.

Consequently, the conclusion emerging from the above discussion is that Li-ion batteries should not operate at currents which are too high, since the surface films on the electrodes and even the bulge of the active mass cannot accommodate the fast volume changes. Nonetheless, starting from their fully charged state, Li-ion batteries should not operate at rates, i.e. currents, that are too low, which cause them to remain in their most unstable situation for too long. Namely, they remain nearly fully charged in a dynamic situation (i.e. a weaker passivation due to the flow of current, while the driving forces of the detrimental side effects are still close to maximum).

Hence, an optimal discharge current,  $I_{OPT}$ , should be defined for a battery, calculated from the  $I_{OPT}$  value of the individual cells. The definition of  $I_{OPT}$  is not trivial. It is specific for each battery system and has to be determined experimentally.

### 3.3. Penalty function

Based on the claims presented in Section 3.2, we define a penalty function. Recall the main claims: (i) an optimal discharge current exists and (ii) other discharge currents, i.e. too high or too low, have negative effects on the battery's life. For each discharge current the function defines a penalty, which is aggregate over time, in terms of damage to the battery's life. The accurate penalty function depends on the specific chemistry of the battery. Nevertheless, we assume that for any chemistry the following basic assumptions hold:

1. The penalty of no discharge is 0.
2. The penalty of the optimal discharge current  $I_{OPT}$ , i.e. the current which results in maximization of the battery's life, is 0.
3. All other discharge currents have positive penalty values proportional to the distance from  $I_{OPT}$ .

We assume the following linear penalty function, presented in Fig. 1. Let  $I$  be the discharge current, then, for some parameter  $\alpha > 0$ ,

$$Penalty(I) = \begin{cases} 0, & \text{if } I = 0 \text{ or } I = I_{OPT} \\ \alpha|I_{OPT} - I| & \text{else} \end{cases} \quad (2)$$

By simple normalization of all demands and capacities, we assume throughout this paper, without loss of generality, that  $I_{OPT} = 1$  and  $\alpha = 1$ .

## 4. Switching algorithms

We present three discharge algorithms: naive in Section 4.1 and two heuristic algorithms in Sections 4.2 and 4.3. The inputs of the

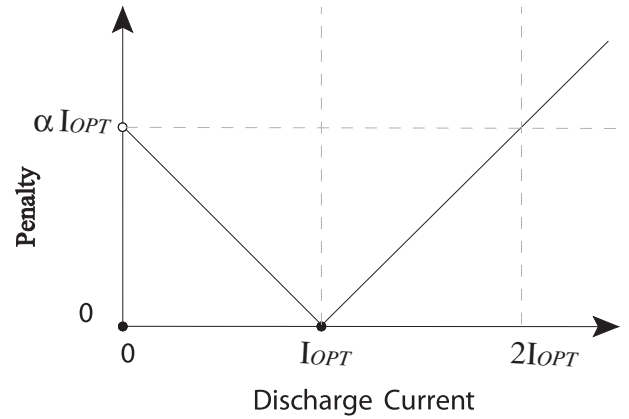


Fig. 1. The penalty function. The plot presents the damage to the battery's life as a function of the discharge current. It is based on the claim that an optimal discharge current exists, whereby other discharge currents, i.e. too high or too low, have negative effects on the battery's life.

algorithms are the cell-series statuses,  $c_j^i$  values, i.e. their remaining capacities, and the current demand,  $d_i$ . The output of the algorithms is the current values allocated to the demand by the cell-series,  $I_j^i$  values. For simplicity, as our algorithms refer to a single demand at a given time,  $d_i$ , we drop the index  $i$  whenever it is clear from the context. Specifically,  $d$  is the demand,  $c_j$  is the remaining capacity of cell-series  $s_j$  before the demand, and  $I_j$  is the current allocated to the demand by cell-series  $s_j$ .

### 4.1. Naive

The naive algorithm, denoted *Naive*, is presented in Algorithm 1. This algorithm is the discharge method commonly used for EV batteries. In this method the current demand is supplied using all the cell-series in the battery simultaneously, so the load is equally divided among them.

The rationale behind this method is simplicity of implementation, i.e. parallel connection of the cell-series. In this algorithm the balancing of the cell-series' capacities is critical since the cell-series are always connected to each other. In case of imbalance of the cell-series, due to their constant parallel connection, a self-discharge and charge between the cell-series will occur, i.e. the most charged cell-series will be discharged in order to charge the emptiest cell-series.

This algorithm is also based on the assumption that the lower the current drawn from each cell-series in the battery the better. As described in Section 3.2, the behavior and performance of a real battery is more complex, and this assumption is not always true.

We present this algorithm as a benchmark for the two other novel algorithms provided in this section.

#### Algorithm 1. Naive

- Require:** Current demand,  $d$ , and cell-series' capacities,  $c_1 \geq \dots \geq c_m$
- 1: Set  $I_j = d/m$  for all cell-series, i.e. for all  $j \in \{1, 2, \dots, m\}$
  - 2: **return**  $I = (I_1, \dots, I_m)$

### 4.2. PreferOPT algorithm

The *PreferOPT* algorithm is presented in Algorithm 2. This is a heuristic algorithm that tries to allocate  $I_{OPT}$  values from the cell-series as much as possible, and allocates the remaining current demand in a way that balances the cell-series' states.

The algorithm can be split into two parts. In the first part, as the name of the algorithm indicates, it assigns  $I_{OPT}$  to the most charged cell-series as long as possible and necessary, lines 2–6. The second part handles the cases of remaining current demand that need to be supplied. Such situations can be relevant in cases where the current demand is not a multiplication of  $I_{OPT}$  or there are not enough cell-series with a remaining capacity of  $I_{OPT}$ .

There are two cases of remaining current demand: a small amount, i.e. less than  $I_{OPT}$ , and a large amount, i.e. more than  $I_{OPT}$ . The small amount is handled in lines 7–11 where two options are considered and the one with the lowest penalty is chosen. The large amount is handled in lines 12 and 13 where the current is supplied from all the cell-series.

#### Algorithm 2. PreferOPT Algorithm

**Require:** Current demand,  $d$ , and cell-series' capacities,  $c_1 \geq \dots \geq c_m$

- 1: index = 1
- 2: **while**  $d \geq I_{OPT}$  **and** index  $\leq m$  **and**  $c_{\text{index}} \geq I_{OPT}$  **do**
- 3: Allocate  $I_{OPT}$  form cell-series  $s_{\text{index}}$ ,  $I_{\text{index}} = I_{OPT}$
- 4: Update remaining current demand,  $d = d - I_{OPT}$
- 5: index = index + 1
- 6: **end while**
- 7: **if**  $0 < d < I_{OPT}$  **then** //small amount remaining
- 8: Consider allocating the remaining current demand  $d$  by:
- 9: (i) CALL *BalancedDischarge* with  $d$  and the subset of all cell-series that were already selected to supply the demand, i.e.  $s_1, \dots, s_{\text{index}}$   
Denote the return vector  $I^{\text{used}}$
- 10: (ii) CALL *BalancedDischarge* with  $d$  and the subset of all cell-series that still have **not** been selected to supply the demand, i.e.  $s_{\text{index}+1}, \dots, s_m$   
Denote the return vector  $I^{\text{new}}$
- 11: Check which allocation vector,  $I^{\text{used}}$  or  $I^{\text{new}}$ , is associated with less penalty and update  $I$  according to it
- 12: **else**  $\{d \geq I_{OPT} - \text{large amount remaining}\}$
- 13: CALL *BalancedDischarge* to allocate the remaining current demand,  $d$ , using all cell-series  $s_1, \dots, s_m$
- 14: **end if**
- 15: **return**  $I = (I_1, \dots, I_m)$

In several places the *PreferOPT* algorithm calls *BalancedDischarge* with a demand and a subset of cell-series. The algorithm *BalancedDischarge*, presented in Algorithm 3, allocates the demand,  $d'$ , in a balancing way among the subset of cell-series,  $c_{\ell+1} \geq c_{\ell+2} \geq \dots \geq c_{\ell+k}$ . That is, the current is allocated from the cell-series in the subset while trying to equalize the remaining capacities in the set after the allocation. This can be done by first allocating from  $s_{\ell+1}$ , till  $c_{\ell+1} = c_{\ell+2}$ , then allocating evenly from both  $s_{\ell+1}, s_{\ell+2}$ , and so on, until the whole demand is allocated. The aim of this discharge allocation is to minimize the capacities' gap between the most charged and most empty cell-series in the set.

#### Algorithm 3. BalancedDischarge

**Require:** Current demand,  $d'$ , and subset of  $k$  cell-series with their capacities,  $c_{\ell+1} \geq c_{\ell+2} \geq \dots \geq c_{\ell+k}$

- 1: Initialize  $I'_j$  values to 0 for all  $j \in \{\ell + 1, \ell + 2, \dots, \ell + k\}$
- 2: index = 1
- 3: **while**  $d' > 0$  and index  $< k$  **do**
- 4: Set  $\Delta = c_{\ell+\text{index}} - c_{\ell+\text{index}+1}$
- 5: **for all** cell-series  $s_j \in \{s_{\ell+1}, \dots, s_{\ell+\text{index}}\}$  **do**
- 6: Update  $I'_j = I'_j + \min\{\Delta, d'/\text{index}\}$
- 7: **end for**

- 8: Update remaining current demand,  $d' = d' - \text{index} \times \min\{\Delta, d'/\text{index}\}$
- 9: index = index + 1
- 10: **end while**
- 11: **return**  $I'_{\ell+1}, I'_{\ell+2}, \dots, I'_{\ell+k}$

A simple demonstration of the *PreferOPT* algorithm is provided below. Assume there are 3 cell-series with  $I_{OPT} = 1$  each with an initial capacity of  $C = 2$ , i.e. (2,2,2), and a demand sequence of 1, 2.4 and 2.6.

The first demand for a current is 1. A demand of 1 unit will be supplied using the first cell-series and the remaining demand will be 0. Thus, the solution vector for this demand will be  $I = (1,0,0)$ , which is associated with a penalty of 0 as there is only an optimal current allocation.

The second demand for a current is 2.4, while the remaining cell-series' capacities, sorted in a decreasing order, are (2,2,1). A demand of 2 units will be supplied using the first two cell-series, one by each, and the remaining demand will be 0.4. The value 0.4 is a small amount for which two options are considered (lines 9 and 10). The first option (line 9) results in the allocation vector (1.2,1.2,0) while the second option (line 10) results in the allocation vector (1,1,0.4). The first allocation vector has a lower penalty since  $0.4 = 2 \times \text{Penalty}(1.2) < \text{Penalty}(0.4) = 0.6$ . Thus, the remaining demand will be supplied using the most charged cell-series that was already selected to supply  $I_{OPT}$ , i.e. using the first two cell-series. Over all, the solution vector for this demand will be  $I = (1.2,1.2,0)$ , which is associated with a penalty of 0.4.

The third, and last, demand for a current is 2.6 while the remaining cell-series' capacities are (1,0.8,0.8). A demand of 1 unit will be supplied using the first cell-series and the remaining demand will be 1.6. No additional  $I_{OPT}$  values can be supplied since all other cell-series' capacities are below  $I_{OPT}$ . The remaining demand, i.e. 1.6, is a large amount (line 12). Thus, the demand will be supplied using all cell-series in a balancing way. Over all, the solution vector for this demand will be  $I = (1,0.8,0.8)$  which is associated with a penalty of  $2 \times \text{Penalty}(0.8) = 2 \times 0.2 = 0.4$ .

The total penalty associated with the entire demand sequence is  $0 + 0.4 + 0.4 = 0.8$ . For comparison, the *Naive* algorithm would have allocated the values 2.1/3, 1.8/3, 2.1/3 for each of the cell-series, respectively for each of the demands. Such allocations would result in a total penalty of  $3 \times [\text{Penalty}(0.7) + \text{Penalty}(0.6) + \text{Penalty}(0.7)] = 3 \times [0.3 + 0.4 + 0.3] = 3$ . In other words, on the specific presented sequence, the *PreferOPT* algorithm eliminates more than 70% of the penalty compared to *Naive*.

#### 4.3. EqualLoad algorithm

The *EqualLoad* algorithm is presented in Algorithm 4. The algorithm searches for the lowest penalty solution that supplies the demand using the same allocation value for all the cell-series.

All the possible subsets of the most charged cell-series are considered. There are only  $m$  options for such subsets, i.e. subset of the most charged cell-series, subset of the two most charged cell-series, and so on up to the subset of all the cell-series. For each option, i.e. subset of the  $k$  most charged cell-series, an assignment similar to that of the *Naive* algorithm is used. In other words, the demand is split equally among all the cell-series in the subset, i.e.  $I_j = d'/k$  for all  $j \in \{1, 2, \dots, k\}$ . Note, if at least one of the cell-series capacity in the subset is not enough, i.e.  $c_j < I_j = d'/k$ , the solution is not feasible and will be ignored. The penalty of each option is calculated and the one with the minimal penalty is chosen.

**Algorithm 4.** EqualLoad Algorithm

**Require:** Current demand,  $d$ , and cell-series' capacities,  $c_1 \geq \dots \geq c_m$

- 1: Initialize solution vector  $I^{\text{best}} = (I_1^{\text{best}}, I_2^{\text{best}}, \dots, I_m^{\text{best}}) = (0, 0, \dots, 0)$
- 2: Initialize BestPenalty =  $\infty$
- 3: **for all** sizes of subset, i.e.  $m' \in \{1, 2, \dots, m\}$  **do**
- 4:   Set  $I_j = d/m'$  for all  $j \in \{1, 2, \dots, m'\}$
- 5:   **if** Penalty( $I$ ) < BestPenalty **and**  $I$  is feasible, i.e.  $\forall j: I_j \leq c_j$  **then**
- 6:      $I^{\text{best}} = I$
- 7:     BestPenalty = Penalty( $I$ )
- 8:   **end if**
- 9: **end for**
- 10: **return**  $I^{\text{best}} = (I_1^{\text{best}}, I_2^{\text{best}}, \dots, I_m^{\text{best}})$

**5. Simulation data**

We evaluated our proposed switching algorithm using computer simulations. The current demands were simulated using the main world-wide driving cycles used in the United States, Europe and Japan [26–28]. Below is a list of the driving cycles we used with a short description of their purpose (sources: [26,29]).

*United States driving cycles:*

- The Urban Dynamometer Driving Schedule (UDDS), also called FTP-72 (Federal Test Procedure) or LA-4 cycle or FUDS, was developed by the United States Environmental Protection Agency (EPA) [30] and is used in the USA to simulate urban driving. This driving cycle is also used in Sweden, where it is called A10 or the CVS (Constant Volume Sampler) cycle, and in Australia, where it is called the ADR 27 (Australian Design Rules) cycle [26]. In this paper we denote it *USA-Urban*, see Fig. 2(a).
- The US06 Supplemental Federal Test Procedure (SFTP) is used in the USA to simulate aggressive driving. It contains high engine loads, high speeds, high acceleration driving behavior and rapid speed fluctuations. In this paper we denote it *USA-Aggressive*, see Fig. 2(b).
- The Highway Fuel Economy Test (HWFET) was developed by the EPA to simulate highway driving in the USA. In this paper we denote it *USA-Highway*, see Fig. 2(c).
- The California Unified Cycle (UC), also called Unified LA-92, developed by the California Environmental Protection Agency (Cal/EPA) [31], to simulate urban driving in California [32]. Compared to USA-Urban it is more aggressive in speeds, accelerations, etc. In this paper we denote it *LA-Urban*, see Fig. 2(d).
- The New York City Cycle (NYCC) simulates city driving in New York City, i.e. at low speeds with frequent stops. In this paper we denote it *NYC-Urban*, see Fig. 2(e).

*European Union driving cycles:*

- ECE-15 Driving Cycle, also known as UDC, is used in Europe to simulate urban driving. It represents European city driving conditions common in cities like Paris and Rome. In this paper we denote it *Europe-Urban*, see Fig. 2(f).
- The New European Driving Cycle (NEDC), also known as the MVEG-A cycle, is used in Europe to simulate urban and highway driving conditions. It contains ECE-15 driving cycles in addition to some aggressive and high speed driving segments. In this paper we denote it *Europe-Urban-Highway*, see Fig. 2(g).

*Japan driving cycle:*

- The 10-15 Mode Cycle is used in Japan to simulate urban driving. It represents low and high speed urban driving. In this paper we denote it *Japan-Urban*, see Fig. 2(h).

The driving cycles, consisting of velocity–time measurements in 1 s intervals, are standardized driving patterns used for measuring the fossil fuel emission and consumption of vehicles. The driving cycles' velocity–time plots are presented in Fig. 2. Notice the x-axis as well as the y-axis in the figure may differ from one plot to another as the duration and the maximum speed of the driving cycles are different.

Due to lack of other alternatives, these driving cycles can be used to evaluate electric power consumption of EV vehicles as well. We converted the velocity–time data into power–time data, assuming a vehicle weighs 1.5 tons and other parameters such as engine efficiency, drivetrain efficiency, air density, coefficient of drag. The conversion process is detailed in Ref. [33]. As explained earlier in Section 3, for simplicity we assume a constant voltage of 360 V during operation as an approximation. In such cases, the power–time data can be converted to current–time data. This was indeed done herein and the converted current–time curves relating to the velocity–time plots of Fig. 2, are presented in Fig. 3. A statistical summary of the current–time data can be found in Table 2.

The conversion process output consists of current–time data which also contains negative current values. These values represent generated current, for instance from braking. Since we do not consider charging in this paper, these negative current values were ignored and they were considered as demands of 0 current.

We used the converted current data of each driving cycle as the current demands. Since we assumed a penalty function which is not affected by the cycle number or the battery age, and since the penalty is aggregate over all discharges during the battery's life, a comparison of the algorithms' performances for only one full discharge cycle is sufficient. Repeating the same discharge cycle over and over again will result in the same outcome. Notice that, in contrast to this methodology, for laboratory testing we would have had to test many discharge cycles, i.e. till the battery would have died, since the affects on the battery after one cycle might not be measurable.

As for the configurations of the battery pack, we checked configurations of packs with different quantities of cell-series starting at 10 up to 700 with intervals of 10, i.e.  $m \in \{10, 20, \dots, 700\}$ .

As an example, in a battery pack of a standard EV that contains 36 kW h, which can enable driving 150–200 km between charging, the number of cell-series is 40. For effective electrical operation of the car, a high voltage of 360 V is needed, which means that each battery series should include 97 cells. Given this voltage, in order to provide 36 kW h, such a battery needs a capacity of 100 A h. If each cell has a capacity of about 2.5 A h, the battery should include 40 series of cells, i.e. a total of nearly 4000 individual cells. However, we simulate battery packs with a varied number of cell-series as it is relevant also to other EV configurations such as heavy duty electric vehicles and even other domains such as grid load leveling.

The total amount of energy was always equal to the total energy required by the tested driving cycle. The initial capacity of all the cell-series in each configuration was the same and equal to the total demand of current, divided by the number of cell-series, i.e.  $C = (\sum_{i=1}^n d_i)/m$ . The optimal discharge current, i.e.  $I_{\text{OPT}}$ , was set to 1 and the penalty function was similar to that presented in Fig. 1 with  $\alpha = 1$ .

**6. Simulation results**

The presentation of the results is divided into two. First we present the penalty of the proposed heuristic algorithms compared to the

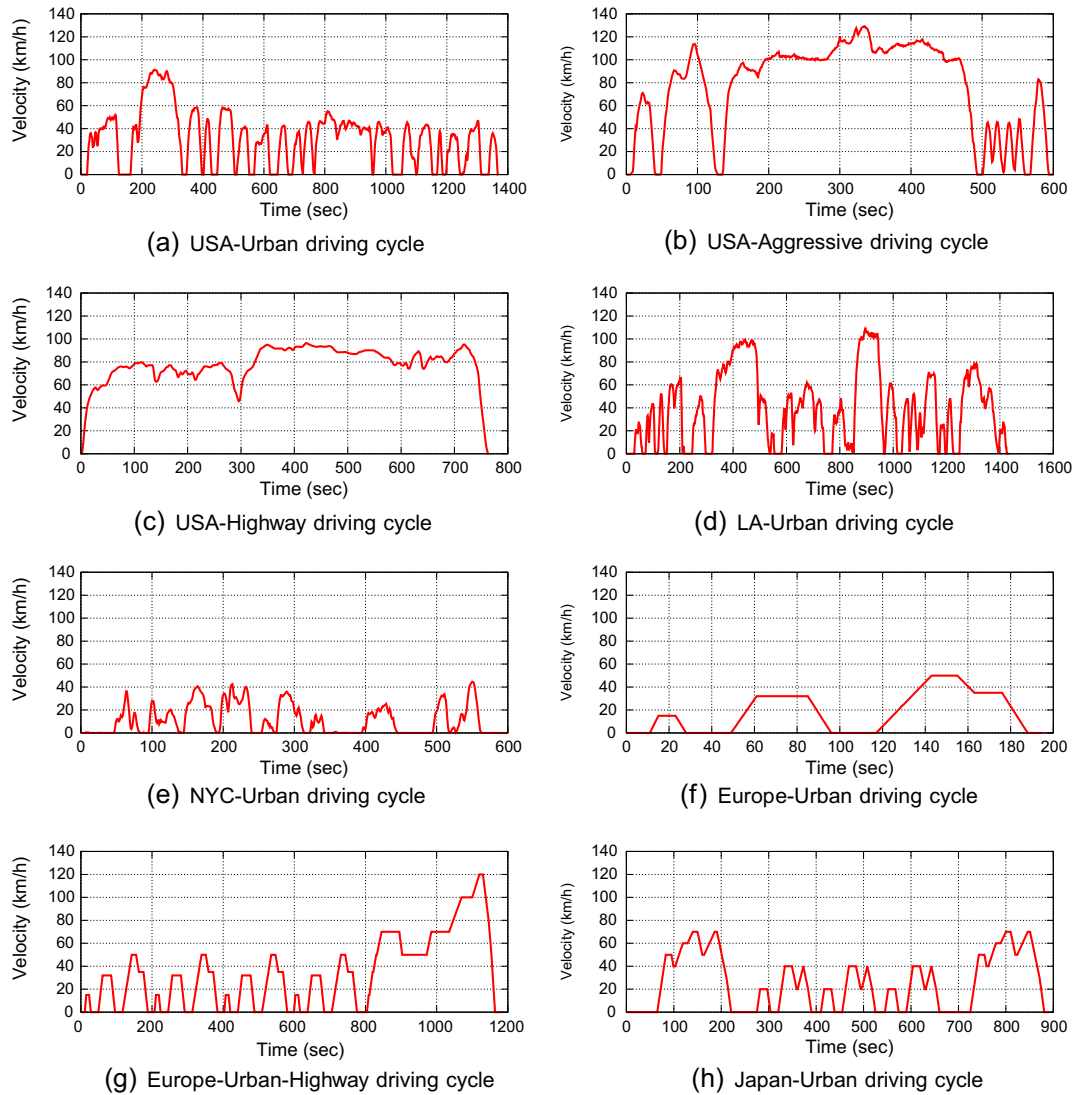


**Fig. 2.** Driving cycles: velocity–time plots. Different data sets of world-wide standardized driving patterns used in the United States, Europe and Japan. The data presented in the plots is velocity, in kilometers per hour (km/h) units, as a function of time, in 1 second (s) intervals.

naive algorithm which is used as a benchmark. Later we describe the differences between the performances of the proposed algorithms.

In general, apparently when using the proposed algorithms the penalty can be significantly reduced and almost totally avoided as the number of cell-series increases. In Fig. 4 the penalties of the *EqualLoad* algorithm compared to the penalties of the *Naive* algorithm are presented as a function of the number of cell-series. The values are *EqualLoad* penalty divided by *Naive* penalty, e.g. a value of 0.7 means the penalty of *EqualLoad* is 70% of the *Naive* penalty. Note, since our objective is minimization of the penalty, the lower the value in the plot the better. The results for the *PreferOPT* algorithm are similar and thus they are not presented.

As shown in Fig. 4, there is a non-linear improvement for almost all driving cycles and as the number of cell-series increases the improvement is better, i.e. the total penalty is lower. This behavior is reasonable and can be explained easily. As the number of cell-series increases there are more switching options and more penalties can be avoided.

For the case of only 10 cell-series there is almost no improvement at all, as expected since there is no room for switching. Already in the case of 50 cell-series there is a significant improvement for NYC-

Urban and Europe-Urban driving cycles, i.e. 80% and 70% of *Naive*, respectively; a minor improvement for USA-Aggressive, USA-Highway and LA-Urban driving cycles, i.e. higher than 97% of *Naive*; and a moderate improvement for all the rest, i.e. 90%–95% of *Naive*.

For the cases with higher quantities of cell-series almost all the penalty is avoided comparing to *Naive*. For 250 cell-series the penalty of Japan-Urban, NYC-Urban and Europe-Urban is around 5% of *Naive*; for USA-Urban and Europe-Urban-Highway the penalty is 10%–25% of *Naive*; for LA-Urban and USA-Highway LA-Urban the penalty is 50%–60% of *Naive*; and for USA-Aggressive there is almost no improvement as the penalty is 95% of *Naive*. For USA-Highway the penalty is less than 10% of *Naive* only when there are more than 350 cell-series, and for LA-Urban only when there are more than 450 cell-series.

The cause for these results can be explained by the statistical analysis of the driving cycles' current demands. An analysis of the results reveals a logical connection for most driving cycles between the decrease of the penalty and the average current demand. A decrease of more than 50% of *Naive* is possible using a quantity of cell-series which is at least equal to the average demand value (see Table 2). For example, the average demand of Europe-Urban-

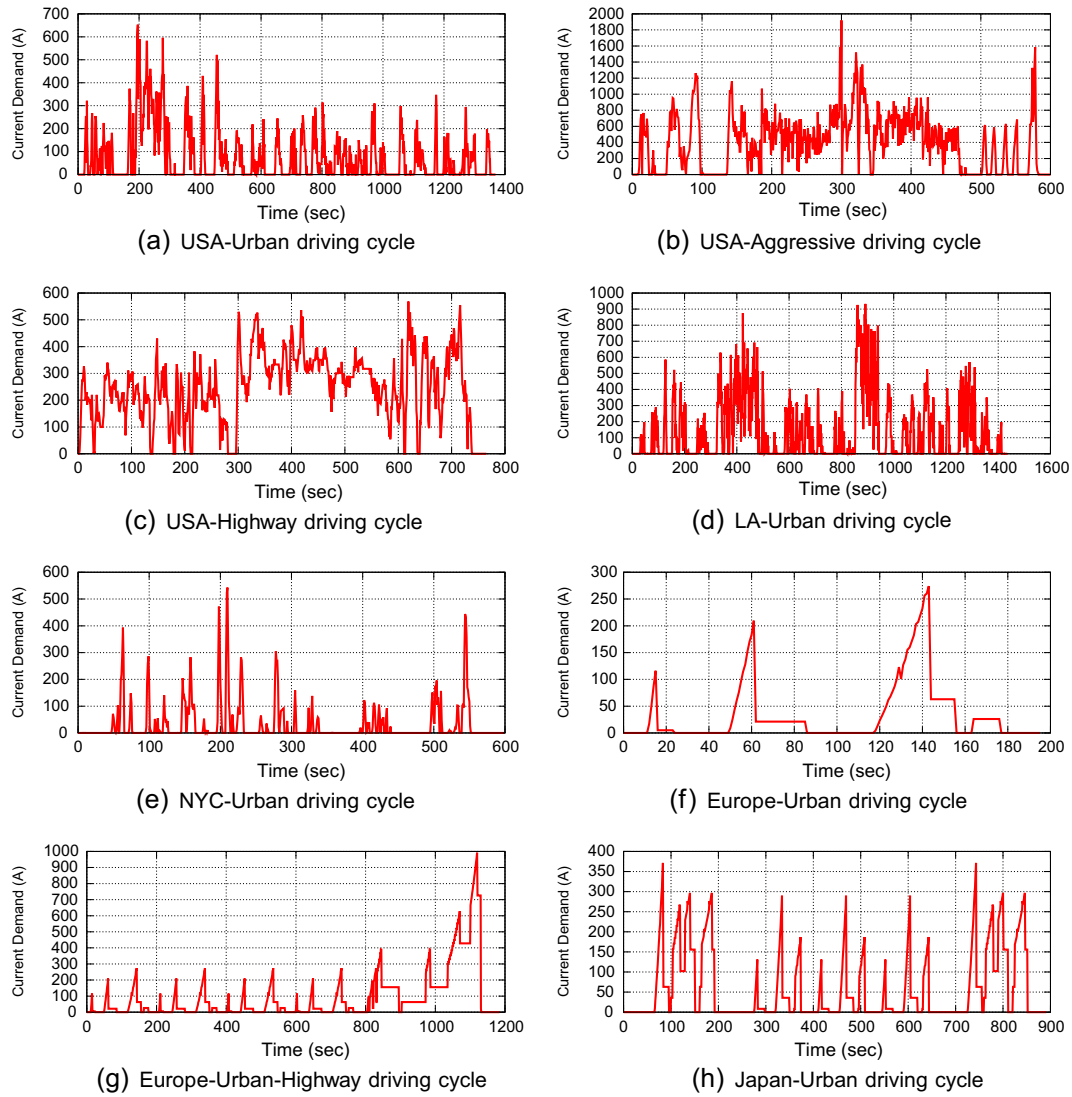


**Fig. 3.** Driving cycles: current–time plots. The velocity–time data from Fig. 2 after conversion to current–time data. The data presented in the plots is current demand, in amperes (A), as a function of time, in 1 second (s) intervals.

Highway is 153 and using 150 cell-series the penalty decreases to a value of approximately 50% of *Naive*. Moreover, by using a quantity of cell-series which is double the average demand value, the penalty can decrease to a value of approximately 10% of *Naive*.

**Table 2**

Statistical summary of the driving cycles' current–time data presented in Fig. 3. Data presented in the columns from left to right: the driving cycle; the total number of demands in the driving cycle; the number of positive demands, i.e. when there is consumption, in the driving cycle; the maximum demand in the driving cycle, in amperes (A); and the average demand in the driving cycle, in amperes (A), taking into account only the positive demands.

Driving cycle	Number of demands		Demand value (A)	
	Total	Positive	Maximum	Average
USA-Urban	1370	768	653	138
USA-Aggressive	601	442	1920	528
USA-Highway	766	698	568	262
LA-Urban	1436	833	933	243
NYC-Urban	599	217	543	90
Europe-Urban	196	99	274	63
Europe-Urban-Highway	1185	715	992	153
Japan-Urban	892	419	371	125

This behavior is reasonable due to the fact that if there are more cell-series than the average demand all the demands lower and equal to the average demand can be supplied at almost no penalty as there are enough cell-series that can supply  $I_{OPT}$  values.

We also compared the penalties of the two heuristic algorithms. In Fig. 5 the penalties of the *PreferOPT* algorithm compared to the *EqualLoad* algorithm are presented as a function of the number of cell-series. For clear presentation, the results are split into two plots. It appears that the *PreferOPT* algorithm outperforms the *EqualLoad* algorithm for most driving cycles. For the aggressive driving cycles, i.e. USA-Aggressive, Europe-Urban-Highway and LA-Urban, seemingly there is no difference between the algorithms for most cases. The *EqualLoad* algorithm outperforms *PreferOPT* only for the Europe-Urban-Highway driving cycle.

**7. Discussion**

In general, the results presented in Fig. 4 imply that by using the proposed heuristics a non-linear penalty reduction is possible for almost all driving cycles. In addition, that as the number of cell-series increases the improvement is better, i.e. the total penalty is

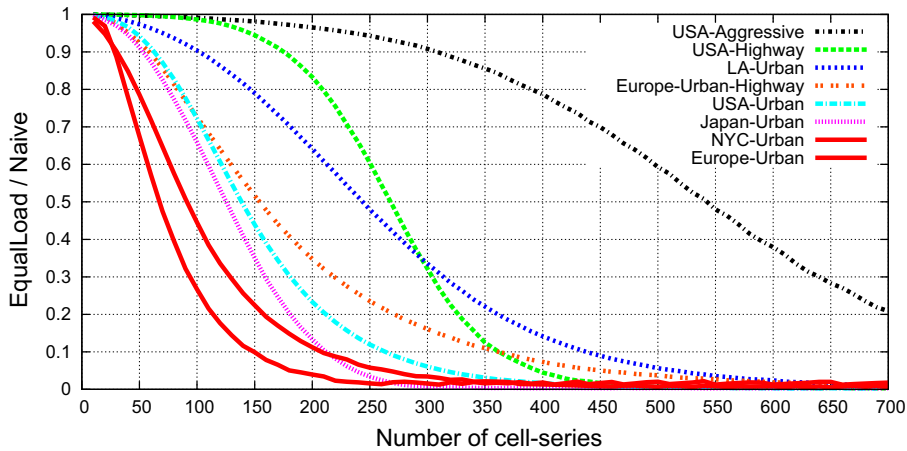


Fig. 4. Improvement in reducing the total penalty: *EqualLoad* algorithm compared to *Naive* algorithm. The lower the value in the plot the better the improvement.

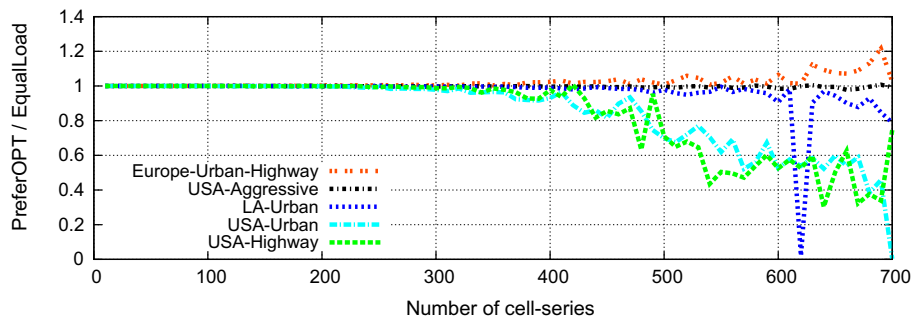
lower. This behavior is reasonable and can be explained easily. As the number of cell-series increases there are more allocation options and more penalties can be avoided.

A statistical analysis of the results and the current demands, reveals connections between the decrease in penalty and the average current demand. A reduction to approximately 50% of *Naive*'s penalty is possible using a quantity of cell-series which is at least equal to the average demand value. For example, as presented in Table 2, the average demand in the Europe-Urban-Highway cycle is 153, whereas using a quantity of 150 cell-series the penalty decreases to approximately 50% of *Naive*'s penalty. Moreover, by using a quantity of cell-series which is double the average current demand value, the penalty decreases to approximately 10% of *Naive*.

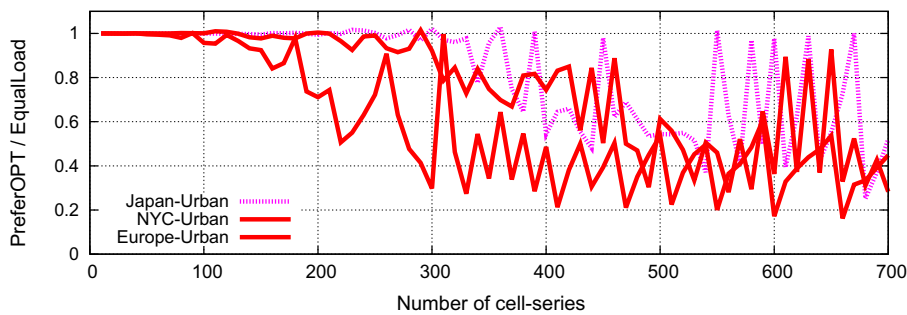
These connections are reasonable. When there are more cell-series than the average demand, most of the demands for lower currents can be supplied at almost no penalty, since there are enough cell-series that can supply  $I_{OPT}$  values. Hence, these connections depend on the value of  $I_{OPT}$ , which is assumed to be 1. However, they can be easily adapted to any other value.

The results in Fig. 5 imply that different heuristics may be preferred for different driving cycles or even for different drivers' behavior. Thus, the current allocation algorithm should be selected based on the relevant driving cycle.

The implementation complexity should also be considered when the proposed algorithms are compared. Implementation of the *EqualLoad* algorithm required a switching circuit with the



(a) Driving cycles: Europe-Urban-Highway, USA-Aggressive, LA-Urban, USA-Urban and USA-Highway.



(b) Driving cycles: Japan-Urban, NYC-Urban and Europe-Urban.

Fig. 5. The penalty of the *PreferOPT* algorithm compared to that of the *EqualLoad* algorithm. A value lower than 1 means that the penalty of *PreferOPT* is lower than that of *EqualLoad*. A value higher than 1 means that the penalty of *EqualLoad* is lower than that of *PreferOPT*.

ability to select a subset of cell-series, where the *PreferOPT* algorithm also required the ability to control the discharge current from each cell-series. Thus, whereas the *PreferOPT* algorithm outperforms *EqualLoad* in most driving cycles, the *EqualLoad* algorithm may be preferred as it is easier to implement.

An in-depth examination of the aggregate penalty along the demand sequence reveals that most of the penalties are obtained at the end of the demand sequence. In other words, most of the penalties are obtained from the demands that arrive when the cell-series are almost empty. These demands turned out to be the most challenging, since the remaining capacity in each cell-series may be small and allocations of the optimal current might not be possible.

Hence, our heuristics seem to perform with minimal damage to the battery's life for a significant prefix of the demand sequence, as long as the remaining capacity of the cell-series is not below some threshold. This property implies that drivers can reduce the penalty even more if they charge their EV frequently enough and do not wait until the battery is empty.

As presented in all result figures, the quantity of the cell-series plays a key role in minimizing the penalty. The more cell-series in the battery the more affective our heuristics. Furthermore, packs with many cell-series allow better safety and better heat management. However, the decision regarding the quantity of cell-series in the battery pack cannot be based only on these aspects. A primary factor that should be considered is the battery's energy density per unit of weight, i.e. the factor that determines the driving distance between full charging processes. As the number of cell-series increases the battery weight increases, and hence the energy density decreases. Consequently, when designing an EV battery pack a compromise should be made while taking into account all aspects.

## 8. Conclusions and future work

A battery's life is greatly affected by the method of use and in this paper we focus on the discharge current. We defined a penalty function to measure the negative effects of discharge in non-optimal discharge currents and presented a switching algorithm that minimizes this function. We proposed switching algorithms that select a subset of the battery's cells for each current demand and control the discharge current from each.

The algorithms were evaluated by simulations on world-wide driving cycles and the preferences were compared to those of the common discharge method where the current demands are supplied using all the cell-series in the battery simultaneously. The results show that the proposed algorithms significantly decrease the total penalty, and for some configurations almost eliminate it. Hence, the battery's life can be extended significantly by the proposed algorithms in comparison to the common discharge method.

There are some interesting questions open for future work. The model can be extended to consider: other parameters, e.g. temperature; mix of non-identical cell-series with different optimal discharge currents; charging opportunities, e.g. for instance energy produced from braking. Another direction for future work is evaluation of the simulation results via laboratory testing of variant battery chemistry.

## References

- [1] J. Van Mierlo, G. Maggetto, P. Lataire, *Energy Conversion and Management* 47 (17) (2006) 2748–2760.
- [2] A. Affanni, A. Bellini, G. Franceschini, P. Guglielmi, C. Tassoni, *IEEE Transactions on Industrial Electronics* 52 (5) (2005) 1343–1349.
- [3] MIT Electric Vehicle Team, *A Guide to Understanding Battery Specifications*, December 2008, <http://mit.edu/evt>.
- [4] M. Delucchi, T. Lipman, *Transportation Research Part D: Transport and Environment* 6 (6) (2001) 371–404.
- [5] F. Laman, K. Brandt, *Journal of Power Sources* 24 (3) (1988) 195–206.
- [6] C. Grosjean, P. Miranda, M. Perrin, P. Poggi, *Renewable and Sustainable Energy Reviews* 16 (3) (2012) 1735–1744.
- [7] J. Gartner, B. Gohn, *Electric Vehicle Batteries*, Tech. Rep., Pike Research, 2012.
- [8] L. Benini, G. Castelli, A. Macii, E. Macii, M. Poncino, R. Scarsi, *Extending Lifetime of Portable Systems by Battery Scheduling*, in: *Proceedings of the Conference on Design, Automation and Test in Europe*, IEEE Press, Piscataway, NJ, USA, 2001, pp. 197–203.
- [9] R. Rao, S. Vrudhula, D. Rakhmatov, *Analysis of Discharge Techniques for Multiple Battery Systems*, in: *Proceedings of the 2003 International Symposium on Low Power Electronics and Design*, ACM New York, NY, USA, 2003, pp. 44–47.
- [10] L. Benini, D. Bruni, A. Macii, E. Macii, M. Poncino, *IEEE Transactions on Computers* 52 (2) (2003) 985–995.
- [11] J.T.B.A. Kessels, M.W.T. Koot, P.P.J. van den Bosch, D.B. Kok, *IEEE Transactions on Vehicular Technology* 57 (2008) 3428–3440.
- [12] M. Koltypin, D. Aurbach, L. Nazar, B. Ellis, *Electrochemical and Solid-State Letters* 10 (2007) A40–A44.
- [13] L. Benini, G. Castelli, A. Macii, R. Scarsi, *IEEE Design & Test of Computers* 18 (2) (2001) 53–60.
- [14] M. Doyle, J. Newman, *Journal of Applied Electrochemistry* 27 (7) (1997) 846–856.
- [15] M. Pedram, Q. Wu, *Design Considerations for Battery-Powered Electronics*, in: *Proceedings of the 36th Annual Conference on Design Automation (DAC'99)*, IEEE Computer Society, Washington, DC, USA, 1999, pp. 861–866.
- [16] W. Mrtle, C.Y. Li, P. Novk, *Journal of the Electrochemical Society* 158 (2011) A1478–A1482.
- [17] P. Verma, P. Maire, P. Novák, *Electrochimica Acta* 55 (22) (2010) 6332–6341.
- [18] E. Peled, D. Golodnitsky, Penciner, *The Anode/Electrolyte Interface*, in: J. Besenhard (Ed.), *Handbook of Battery Materials*, WileyVCH, 1999, p. 419456 (Chapter 6).
- [19] M. Winter, J. Besenhard, M. Spahr, P. Novák, *Advanced Materials* 10 (10) (1998) 725–763.
- [20] D. Aurbach, M. Koltypin, H. Teller, *Langmuir* 18 (23) (2002) 9000–9009.
- [21] D. Aurbach, B. Markovsky, G. Salitra, E. Markevich, Y. Talyossef, M. Koltypin, L. Nazar, B. Ellis, D. Kovacheva, *Journal of Power Sources* 165 (2) (2007) 491–499.
- [22] V. Etacheri, R. Marom, R. Elazari, G. Salitra, D. Aurbach, *Energy and Environmental Science* 4 (9) (2011) 3243–3262.
- [23] D. Aurbach, B. Markovsky, A. Rodkin, Y. Talyossef, G. Salitra, H.J. Kim, *Journal of the Electrochemical Society* 151 (2004) A1068–A1076.
- [24] G. Ning, B. Haran, B. Popov, *Journal of Power Sources* 117 (1–2) (2003) 160–169.
- [25] N. Liu, A. Jansen, J.T. Vaughey, C.M. Lopez, D.W. Dees, W. Lu, *Journal of the Electrochemical Society* 159 (2012) A566.
- [26] DieselNet, *Emission test cycles*, <http://www.dieselnet.com>.
- [27] F. An, A. Sauer, *Comparison of Passenger Vehicle Fuel Economy and Greenhouse Gas Emission Standards Around the World*, Tech. Rep., Pew Center on Global Climate Change, <http://www.c2es.org/>, December 2004.
- [28] E. Tzirakis, K. Pitsas, F. Zannikos, S. Stournas, *Global Nest Journal* 8 (3) (2006) 282–290.
- [29] United States Environmental Protection Agency (EPA), *Testing and Measuring Emissions: Dynamometer Driver's Aid*, <http://www.epa.gov/nvfel/testing/dynamometer.htm>.
- [30] United States Environmental Protection Agency (EPA), <http://www.epa.gov>.
- [31] California Environmental Protection Agency (Cal/EPA), <http://www.calepa.ca.gov>.
- [32] J.R. Holmes, *Driving Patterns and Emissions: A New Testing Cycle*. Research Note 96–11, California Environmental Protection Agency, Research Division, P.O. Box 2815, Sacramento CA 98512, December 1996, <http://www.arb.ca.gov/research/resnotes/notes/96-11.htm>.
- [33] M.J. Safoutin, *Wheels – online road load energy demand calculator*, <http://www.virtual-car.org>.